

Occurrence of negative epsilon in seismic hazard analysis deaggregation, and its impact on target spectra computation

Lynne S. Burks^{*,†} and Jack W. Baker

Department of Civil and Environmental Engineering, Stanford University, Stanford, CA 94305, USA

SUMMARY

This paper investigates circumstances behind the occurrence of negative ε (the normalized difference between the spectral acceleration of a recorded ground motion and the median response predicted by a ground motion prediction equation) in probabilistic seismic hazard deaggregation. Negative ε values are of engineering interest because of their impact on the conditional mean spectrum (CMS), which is a proposed alternative to the uniform hazard spectrum (UHS) as a target spectrum for ground motion selection. In the case where target ε values from deaggregation are positive, the CMS calculation produces relatively lower response spectra than the UHS. Positive target ε values occur almost universally in active seismic regions at long return periods of engineering interest, but the possibility of negative target ε values is important because in the case of negative target ε , some relationships between the CMS and UHS would reverse. This paper describes the calculation of target ε , performs parametric studies to determine when negative ε values occur in deaggregation, and investigates the potential impact on target spectrum calculation and ground motion selection. The case studies indicate that special seismicity models and certain ground motion prediction equations have the most significant effect on ε values and a combination of these characteristics in Eastern North America creates the most likely situation for negative target ε to occur. CMS results are nonintuitive when the target ε is negative, but it is not clear that this is a common practical concern because negative target ε occurs only in well-constrained areas. Copyright © 2011 John Wiley & Sons, Ltd.

Received 3 December 2010; Revised 24 May 2011; Accepted 3 October 2011

KEY WORDS: ground motion selection; uniform hazard spectrum; conditional mean spectrum; negative epsilon; ground motion prediction equation

1. INTRODUCTION

Ground motion selection is the process by which analysts choose ground motions that are representative of the site of interest and is a key step in performance-based earthquake engineering (PBEE). Often, engineers select ground motions that match a target spectrum, in addition to other properties of interest. The target spectrum is frequently a uniform hazard spectrum (UHS), although a conditional mean spectrum (CMS) may be used as an alternative. Typical discussion of this alternative states that the CMS will be lower than the UHS when target ε values from seismic hazard deaggregation are positive [1]. Writing on the topic notes that target ε values are typically positive in practice, but this is not always certain. This section provides some background on determination of target ε values from seismic hazard deaggregation, describes computation of these target spectra, and illustrates the change to current research thinking if negative target ε values occur in situations of engineering interest.

^{*}Correspondence to: Lynne S. Burks, Department of Civil and Environmental Engineering, Stanford University, Stanford, CA 94305, USA.

[†]E-mail: lynne.burks@stanford.edu

1.1. Probabilistic seismic hazard analysis

Probabilistic seismic hazard analysis (PSHA) quantifies seismic hazard at a site by considering the ground motions that could result from all possible earthquake sources around the site, all magnitudes that each source can produce, and all site-to-source distances. The PSHA integral combines these parameters to compute the exceedance rate of a given intensity measure (i.e., spectral acceleration), as shown for a single seismic source below:

$$\lambda(Sa(T) > x) = \lambda(M > m_{\min}) \int_{m_{\min}}^{m_{\max}} \int_0^{r_{\max}} \int_{-\infty}^{\infty} P(Sa(T) > x|m, r, e) f_{M,R,\varepsilon}(m, r, e) dedrdm \quad (1)$$

where $Sa(T)$ denotes spectral acceleration at a given period T ; $P(Sa(T) > x|m, r, e)$ predicts the probability of $Sa(T) > x$ given a magnitude m , distance r and ε value e and comes from a ground motion prediction equation (GMPE, previously known as an attenuation relationship); $f_{M,R,\varepsilon}(m, r, e)$ is the joint probability density function of magnitude, distance and ε ; $\lambda(M > m_{\min})$ is the rate of occurrence of earthquakes greater than m_{\min} from the source; and $\lambda(Sa(T) > x)$ is the rate of $Sa(T) > x$. Note that GMPEs are functions that typically include additional parameters such as faulting mechanism and site conditions, but the dependence on those parameters is omitted here for clarity. In practice, engineers typically use a discretized form of this equation by binning magnitude, distance, and ε , to perform numerical summations rather than integrals.

The term ε in the above equation accounts for the variability in $Sa(T)$ among ground motions with a common earthquake magnitude and distance, and is defined as the number of standard deviations by which a given logarithmic spectral acceleration differs from the predicted mean logarithmic spectral acceleration, as shown in mathematical form in Equation (2) [2]:

$$\varepsilon(T) = \frac{\ln Sa(T) - \mu_{\ln Sa}(M, R, T)}{\sigma_{\ln Sa}(T)} \quad (2)$$

where $\ln Sa$ is the natural logarithm of the given spectral acceleration and $\mu_{\ln Sa}$ and $\sigma_{\ln Sa}$ are the predicted mean and standard deviation of $\ln Sa$ at a given period, magnitude, and distance. Because of the normalization by $\mu_{\ln Sa}$ and $\sigma_{\ln Sa}$ from the GMPE, ε is well represented by the standard normal distribution with an expected value of zero and a unit standard deviation [2].

While PSHA is useful for quantifying the total hazard at a site, sometimes it is necessary to know which combinations of magnitude, distance, and ε are the most likely for design purposes. Deaggregation is a technique used to find the distribution of magnitude, distance, and ε given exceedance of a certain intensity measure (i.e., $Sa(T)$) [3]. For example, Equation (3) shows the mathematical form of magnitude deaggregation:

$$P(M = m|Sa(T) > x) = \frac{\lambda(Sa(T) > x, M = m)}{\lambda(Sa(T) > x)} \quad (3)$$

where $P(M = m|Sa(T) > x)$ is the probability that magnitude is equal to m given that the spectral acceleration has exceeded x , $\lambda(Sa(T) > x, M = m)$ is the rate of earthquakes that exceed spectral acceleration x and have magnitude equal to m , and $\lambda(Sa(T) > x)$ is the rate at which spectral acceleration exceeds x and this term comes from Equation (1). Deaggregation on distance and ε is computed in the same way, with the appropriate variable replacing magnitude in the above equation. Similarly, joint distributions can be computed using deaggregation, as shown in the following equation for magnitude and ε :

$$P(M = m, \varepsilon = e|Sa(T) > x) = \frac{\lambda(Sa(T) > x, M = m, \varepsilon = e)}{\lambda(Sa(T) > x)} \quad (4)$$

where $P(M = m, \varepsilon = e|Sa(T) > x)$ is the probability that magnitude is equal to m and ε is equal to e given that the spectral acceleration has exceeded x ; $\lambda(Sa(T) > x, M = m, \varepsilon = e)$ is the rate of

earthquakes that exceed spectral acceleration x , have magnitude equal to m , and ε equal to e ; and $\lambda(Sa(T) > x)$ is the rate that spectral acceleration is exceeded from the PSHA integral (Equation (1)).

Deaggregation can also be conditioned on the occurrence of an intensity measure, rather than the exceedance, as shown in the following equation for magnitude and ε [4]:

$$\frac{P(M = m, \varepsilon = e | Sa(T) = x_i) = P(M = m, \varepsilon = e | Sa(T) > x_{i-1})P(Sa(T) > x_{i-1}) - P(M = m, \varepsilon = e | Sa(T) > x_{i+1})P(Sa(T) > x_{i+1})}{P(Sa(T) > x_{i-1}) - P(Sa(T) > x_{i+1})} \tag{5}$$

where $P(M = m, \varepsilon = e | Sa(T) > x_{i \pm 1})$ is a joint deaggregation on magnitude and ε given that spectral acceleration exceeds $x_{i \pm 1}$ and $P(Sa(T) > x_{i \pm 1})$ is the probability that spectral acceleration exceeds $x_{i \pm 1}$. These terms are needed for two values of spectral acceleration: one greater than and one less than the spectral acceleration amplitude of interest.

1.2. Uniform hazard spectrum

Engineers often use the uniform hazard spectrum (UHS) in seismic analysis. This spectrum is obtained by performing PSHA calculations for spectral accelerations with varying periods and identifying the Sa amplitude at each period with the same rate of exceedance. The constant exceedance rate of each period is the source of the name ‘uniform hazard.’ A real ground motion, which has a ‘bumpy’ response spectrum, has ε values that vary with period. That bumpiness is not captured by the UHS, however, because of the independent analyses performed at each period. To illustrate, consider a hypothetical site where the only possible nearby earthquake event is a magnitude 7 earthquake at a distance of 15 km, occurring at a mean rate of once every 75 years. In this case, magnitude and distance are fixed and ε is the only free variable in PSHA. Therefore, variation in a ground motion’s spectral acceleration with period will be due only to variation of ε , and to obtain a ground motion with a lower rate of exceedance, one must have a ground motion with a higher (i.e., rarer) ε . In this case, the UHS with a 10% probability of exceedance in 50 years will consist of spectral acceleration values with $\varepsilon(T) = 1$ as defined by Equation (2), because the standard normal distribution of ε implies that $P(\varepsilon(T) > 1) = 0.159$. Thus, in this simplified analysis case $\lambda(Sa(T) > x) = \lambda(M > m_{\min}) * P(\varepsilon(T) > 1) = 1/75 * 0.159 = 0.0021$, corresponding to a 10% probability of exceedance in 50 years. Looking more generally at this calculation, we can infer that positive ε values will be associated with Sa amplitudes that are rare relative to the rate of occurrence of earthquake events contributing most to exceedance of the given Sa ; this will be explored further in the calculations that follow.

See Figure 1 for a comparison of the UHS and median response spectrum for this case, and notice that the UHS remains at a constant one standard deviation from the median response spectrum at all periods. (Note that here and later, ‘median spectrum’ refers to the exponential of the mean

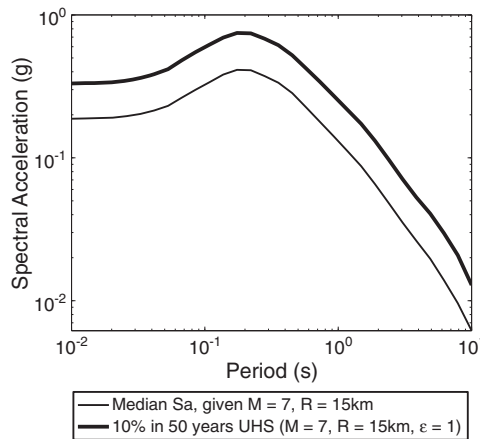


Figure 1. Uniform hazard spectrum shown in comparison with the median response spectrum.

$\ln Sa, \mu_{\ln Sa}$.) The UHS can be considered conservative because given the occurrence of the earthquake, the rate of observing an $\varepsilon > 1$ at all periods is much lower than the rate of observing an $\varepsilon > 1$ at any single period. The conservative nature of the UHS is well appreciated in the earthquake engineering community because it represents an envelope of all possible earthquakes around a site and can suggest impossible earthquake scenarios [5–7]. While this conservatism is acceptable or perhaps even desirable in some situations such as code checks, it is undesirable in other cases. For example, the expected structural response is required to compute an estimate of the expected financial losses because of damage following an earthquake. The use of the UHS to select ground motions could lead to an over prediction of the response and resulting loss, leading to incorrect decisions regarding insurance pricing or decision-making to retrofit the structure.

1.3. Conditional mean spectrum

The conditional mean spectrum (CMS) is a proposed alternative target spectrum that avoids the enveloping problems associated with the UHS [1]. When compared with other ground motion selection techniques in a recent study, selecting ground motions based on their match with the CMS is found to be an accurate and precise selection method that avoids the conservatism of the UHS [8]. The CMS is computed by choosing a period of interest, denoted T^* , (often, but not necessarily, the first mode period of the structure of interest) and the associated amplitude of spectral acceleration, x , then finding the mean ε associated with $Sa(T^*) = x$ from deaggregation. The mean $\ln Sa$ (or equivalently, median Sa) at other periods can be computed using the mean ε associated with $Sa(T^*)$ coupled with a correlation coefficient as shown in the following equation [1]:

$$\mu_{\ln Sa(T_i)} | \ln(T^*) = \mu_{\ln Sa}(M, R, T_i) + \rho(T_i, T^*) \varepsilon(T^*) \sigma_{\ln Sa}(T_i) \quad (6)$$

where $\mu_{\ln Sa}$ and $\sigma_{\ln Sa}$ are the predicted mean and standard deviation of $\ln Sa$ from a GMPE, $\varepsilon(T^*)$ is the mean ε associated with $Sa(T^*) = x$ from deaggregation, and $\rho(T_i, T^*)$ is a correlation coefficient computed using, for example, [9].

An example of the CMS with T^* equal to 1 s can be seen in Figure 2(a). Here, $Sa(T^*)$ is chosen to be the $Sa(1\text{ s})$ value with a 10% probability of exceedance in 50 years at the example site described in the previous section. The CMS is thus equal to the UHS at T^* and is lower than the UHS at all other periods. This is because $\rho(T_i, T^*)$ (the correlation coefficient) for the CMS is less than 1 at all period pairs while the equivalent ρ for the UHS is essentially equal to 1 at all periods (because ε at all periods is equal). From this figure, it is clear that when ε is positive, the UHS is conservative and designers may benefit from using the CMS.

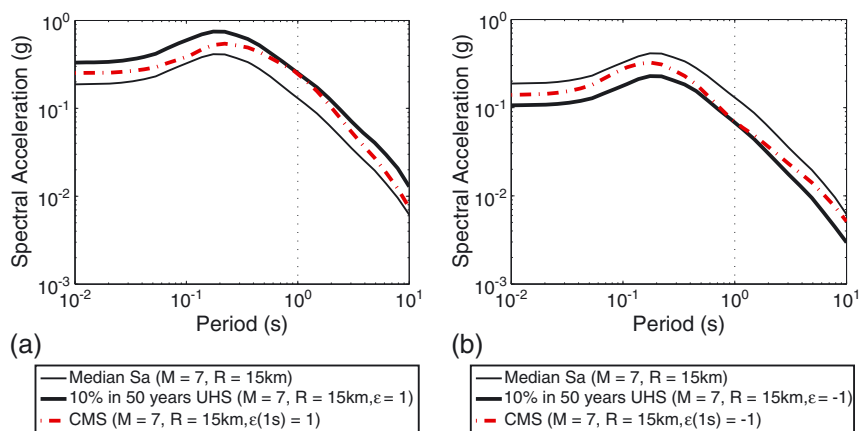


Figure 2. Conditional mean spectrum shown in comparison with the UHS and the median response spectrum with: (a) positive ε and (b) negative ε .

1.4. Negative epsilon

When ε is positive, the CMS predicts less intense response spectra than the UHS, which is partially why this tool is of interest. However, one concern about the CMS that has not been addressed is the possibility of encountering negative target ε in practical engineering analysis. The US Geological Survey (USGS) produces deaggregation maps (discussed below) that show regions where negative ε occur, indicating that this is a legitimate concern. In the event of a negative ε , the CMS would predict a larger response than the UHS as shown in Figure 2(b), which shows a CMS for the example site when $\varepsilon(1\text{ s}) = -1$. As the spectrum moves away from T^* , ε values become larger (i.e., closer to zero) and the CMS moves toward the median response spectrum. Because the median response spectrum is larger than the UHS when ε is negative, the CMS also predicts a larger response.

1.5. Existing epsilon deaggregation maps

Modal ε deaggregation maps associated with USGS hazard calculations for Eastern North America (ENA) have been created by Harmsen [10] and are shown in Figure 3. The map on the right shows the deaggregation for a PGA exceeded with 10% probability in 50 years. There are large regions of negative ε centered over the New Madrid Seismic Zone (NMSZ), eastern Tennessee, and Charleston, SC. No such negative ε regions are observed in the Western United States (WUS).

The USGS documentation of the seismic hazard maps provides some insight into the causes of negative ε in these areas [11]. The map shown in Figure 4, which is adapted from that documentation, highlights regions that include special seismicity models. A special seismicity model describes the relative frequency of different earthquake magnitudes using a characteristic earthquake model or a Gutenberg–Richter (GR) distribution with a large minimum magnitude, as opposed to a typical seismicity model that uses a GR distribution with a wide range of magnitudes to describe this frequency [11]. As a result, special seismicity models tend to predict the repeated occurrence of an event with similar magnitude, with relatively little intermittent seismicity. The typical seismicity models, in contrast, predict significantly more small magnitude events. The areas of special seismicity correspond to the regions of negative ε in Figure 3. On the basis of this realization, parametric case studies are described in the following sections to understand more completely under what circumstances these negative ε values arise.

2. CASE STUDIES WITH DEAGGREGATION GIVEN $\text{PGA} > X$

An idealized site modeled loosely on Charleston, SC was created for parametric case studies. The input parameters for this site (seismicity model, GMPE, etc.) were then varied to see how the deaggregation results change.

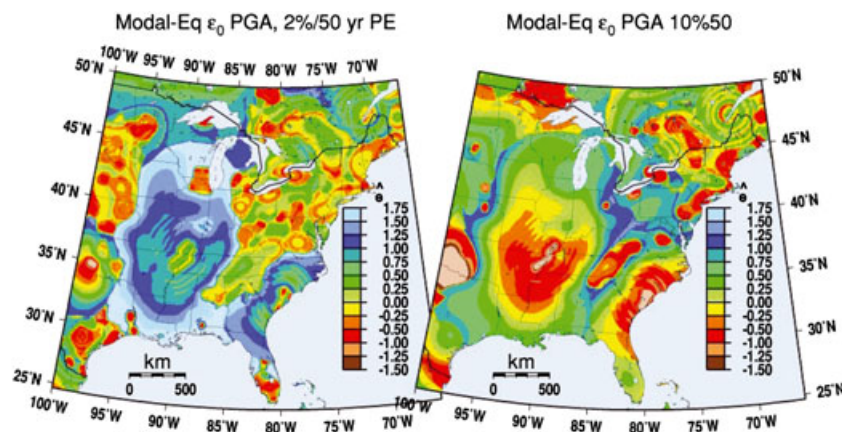


Figure 3. Modal ε deaggregation maps for ENA (from Ref. [10]).

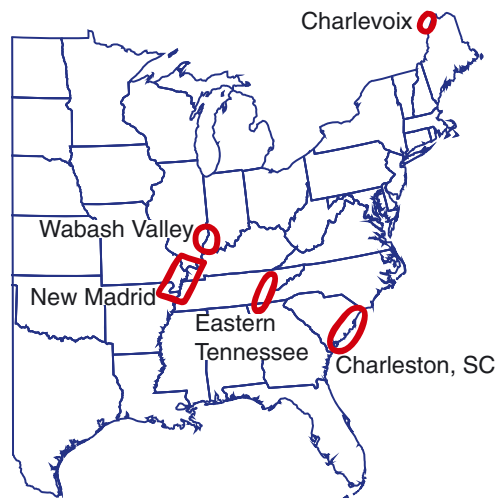


Figure 4. Regions with special seismicity models in the USGS hazard calculations (adapted from Ref. [11]).

2.1. Gutenberg–Richter magnitudes

The initial case study considers a site with a single source at a fixed distance of 15 km, GR distribution of magnitudes, and the Atkinson–Boore ENA GMPE [12]. A GR distribution represents the relative frequency of different earthquake magnitudes from a particular source as shown in the following equation [13]:

$$\log N = a - bM \quad (7)$$

where N is the number of earthquakes of magnitude M or greater per unit of time and a and b are constants. The constant b is typically referred to as the GR slope. N directly relates to the rate of earthquakes at a site, $\lambda(M > m_{\min})$, used in the PSHA integral (Equation (1)). A typical value of b is 1, with values ranging more generally from approximately 0.8 to 1.2. From Equation (7), one can see that when b is decreased, the rate of large magnitude earthquakes increases. In all calculations below, b is equal to 1 unless otherwise noted.

Figure 5 shows magnitude and ε deaggregations for the idealized site described previously and for a PGA (which is equivalent to S_a at $T=0$ s) greater than $0.2g$ and $1.0g$. For exceedance of a small amplitude PGA in Figure 5(a), the deaggregation is dominated by earthquake magnitudes from 5 to 6 and by positive ε values from 1 to 2. There is some probability of negative ε associated with large magnitudes, but it is very small. For exceedance of a large amplitude PGA in Figure 5(b), the deaggregation shows that all magnitudes contribute to exceedances, but positive ε from 1 to 4 dominate and there is no longer any probability associated with negative ε . These results illustrate

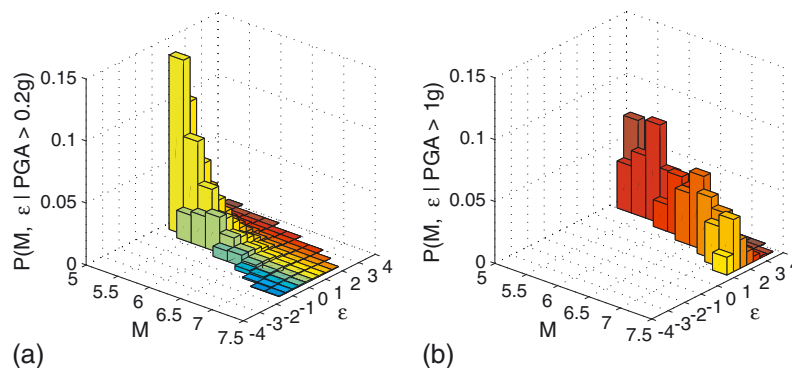


Figure 5. Magnitude and ε deaggregation for an idealized site with (a) $\text{PGA} > 0.2g$ and (b) $\text{PGA} > 1.0g$.

that contributions from negative ε in deaggregation are more likely when considering exceedance of small amplitude PGAs, which is equivalent to considering relatively high probabilities of exceedance.

2.2. Bounding of Gutenberg–Richter magnitudes

When performing PSHA, a minimum and maximum considered magnitude are typically specified. A minimum magnitude of 5 is often used in PSHA for buildings [11], under the assumption that smaller magnitude earthquakes will not cause ground motions intense enough to be of engineering interest. Smaller minimum magnitudes may be used in other cases such as assessment of nuclear facilities [14]. The choice of a minimum magnitude can affect the estimated hazard as shown in Figure 6, which shows several seismic hazard curves computed for the idealized site with varying minimum magnitudes.

By decreasing the minimum magnitude, additional ground motions of small amplitude are considered, causing the seismic hazard curve to shift to higher rates at smaller PGAs. However, as PGA increases, the seismic hazard curves converge because small magnitude events do not contribute to the exceedance of large PGAs.

To see how ε deaggregation changes with minimum magnitude, marginal deaggregation distributions of ε only, given $\text{PGA} > 0.2g$, are shown in Figure 7. As the minimum magnitude increases, the probability of negative ε also increases. The difference between ε deaggregations becomes more dramatic as the minimum magnitude increases, that is, the ε deaggregation for a minimum magnitude of 3 looks fairly similar to a minimum magnitude of 4, but the ε deaggregation for a minimum magnitude of 5 looks very different from a minimum magnitude of 6. These results support the previously stated idea that a special seismicity model consisting of a GR distribution with a large minimum magnitude will be more likely to produce negative ε .

2.3. Characteristic earthquakes

The next idealized site includes characteristic earthquakes in the PSHA calculation. Paleoseismic and other data indicate that certain faults and fault segments may not follow an exponential distribution of magnitudes as indicated by the GR model, but instead tend to produce repeated earthquakes of similar magnitude known as characteristic earthquakes [15]. The characteristic earthquakes included in this analysis occur with a rate of 1/550 per year and have magnitudes and associated probabilities as shown in Table I, following the USGS model for Charleston, SC [11]. The rate of the GR magnitudes is 1/1000 per year and was chosen so that the results here match USGS deaggregation results for Charleston.

Figure 8 shows magnitude and ε deaggregations for the idealized site with characteristic earthquakes for PGA greater than 0.2g and 1.0g. Both deaggregations are dominated by characteristic earthquakes, but again the small PGA amplitude case in Figure 8(a) shows significant probability of negative ε values while the high PGA amplitude in Figure 8(b) shows only positive ε values.

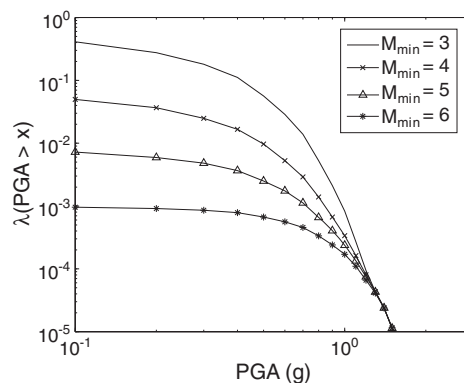


Figure 6. Seismic hazard curve for the idealized site with varying minimum magnitude.

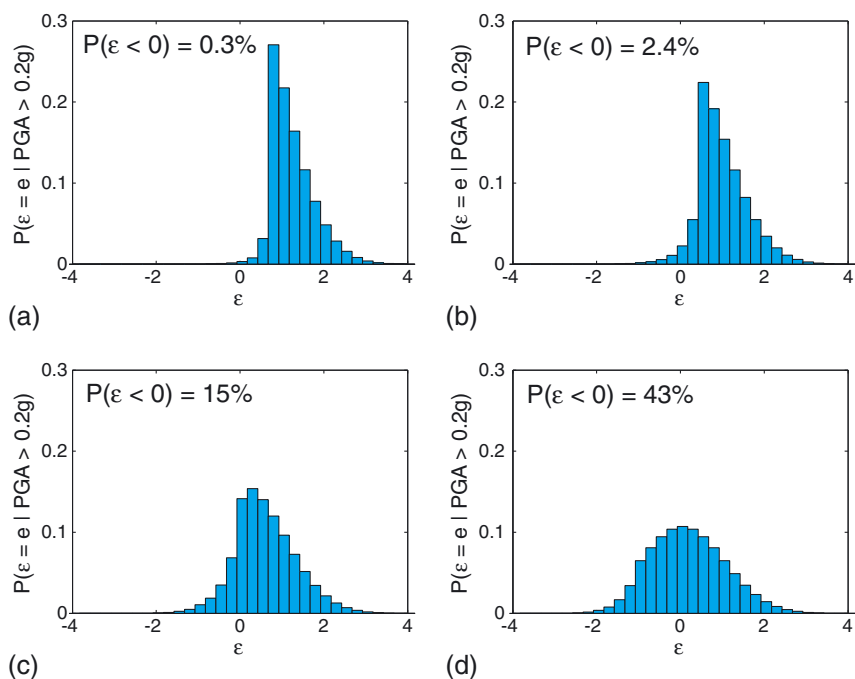


Figure 7. Epsilon deaggregations with a GR magnitude distribution with (a) $m_{\min} = 3$, (b) $m_{\min} = 4$, (c) $m_{\min} = 5$, and (d) $m_{\min} = 6$.

Table I. Magnitude and associated probability of the characteristic earthquakes included in this analysis, which is the same model used by the USGS for Charleston, SC [11].

Magnitude	Probability
6.8	0.20
7.1	0.20
7.3	0.45
7.5	0.15

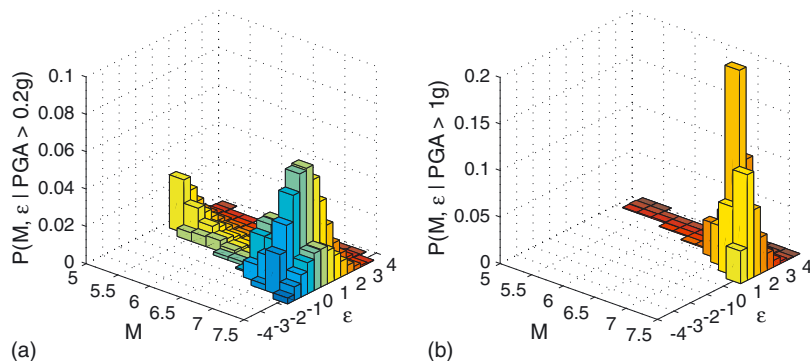


Figure 8. Magnitude and ϵ deaggregation for an idealized site including characteristic earthquakes for (a) $PGA > 0.2g$ and (b) $PGA > 1.0g$.

2.4. Ground motion prediction equations

The following PSHA calculation uses the same seismic source as the previous section (located at 15 km from the site and including both characteristic and GR events), but uses the Boore–Atkinson next generation attenuation (NGA) GMPE developed for the WUS to predict ground motions [16]. Comparing Figure 8(a) (obtained using the ENA GMPE) and Figure 9(a) (obtained using the WUS

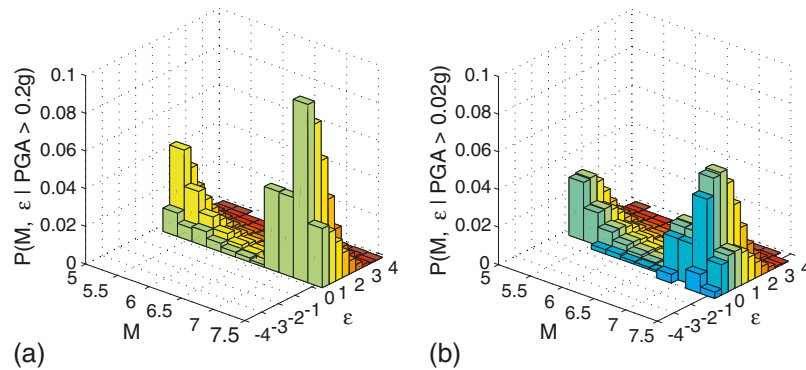


Figure 9. Magnitude and ϵ deaggregation, using the Boore–Atkinson NGA GMPE, (a) given $\text{PGA} > 0.2g$ at distance of 15 km and (b) given $\text{PGA} > 0.02g$ at distance of 0 km.

GMPE), the magnitude deaggregation is similar and is again dominated by characteristic earthquakes, but the ϵ deaggregation is very different. In Figure 8(a) there is a wide distribution of ϵ for a given magnitude and there is a high probability of negative ϵ values. Figure 9(a), however, includes only positive ϵ values. This occurs because the Boore–Atkinson NGA (WUS) model predicts much lower PGA values than the Atkinson–Boore ENA model; so positive ϵ 's are required to reach $0.2g$ even for the largest magnitudes considered. The Boore–Atkinson NGA model can produce negative ϵ values, as shown in Figure 9(b), which shows deaggregation results for $\text{PGA} > 0.02g$ for a site at a distance of 0 km. These negative ϵ values generally appear in this case when considering a small intensity event that is not of engineering interest.

2.4.1. Peak ground acceleration. Figure 10(a) shows how the median predicted PGA changes with variation in magnitude for four different GMPEs (with a constant distance of 15 km and V_{S30} of 310 m/s). The four GMPEs used for comparison are the Atkinson–Boore ENA GMPE [12], Toro *et al.* ENA GMPE [17], Boore–Atkinson NGA GMPE [16], and Campbell–Bozorgnia NGA GMPE [18]. Both the Boore–Atkinson NGA GMPE and the Campbell–Bozorgnia NGA GMPE are calibrated for the WUS and predict a lower median PGA relative to the Atkinson–Boore ENA GMPE and the Toro *et al.* ENA GMPE for large magnitudes. To have a negative ϵ , the engineer must be interested in a PGA amplitude smaller than the predicted PGA, which is unlikely to happen when the predicted PGA is so low. However, the ENA equations predict high PGA values, allowing for the possibility of a negative ϵ .

2.4.2. Spectral acceleration. The conclusion that ENA GMPEs predict higher accelerations than WUS models at large magnitudes extends to spectral accelerations for short period structures. Figures 10(b)–(d) show the same comparison as Figure 10(a) for S_a at periods 0.2 to 1.0 s. At a period of 0.2 s, the difference between the predictions from ENA and WUS equations is even more pronounced than it was for PGA. At a period of 0.6 s, the difference between the equations becomes smaller, and at a period of 1.0 s, the difference is almost negligible.

Another way to view the same data is shown in Figure 11 as the ratio of the predicted spectral acceleration for a magnitude 8 earthquake to a magnitude 5 earthquake as it varies with period (again with a constant distance of 15 km and V_{S30} of 310 m/s). This figure shows how sensitive a given GMPE is to changes in magnitude. At all periods, the ratios for ENA GMPEs are larger than the ratios for WUS GMPEs, indicating that high spectral accelerations are more likely for a given magnitude and therefore negative ϵ 's are more likely.

3. CASE STUDIES WITH DEAGGREGATION GIVEN $\text{PGA} = X$

To simplify the three-dimensional deaggregation figures from the case studies with deaggregation given $\text{PGA} > x$, and to obtain deaggregation results more directly related to CMS calculations, we now consider deaggregation given $\text{PGA} = x$, as computed using Equation (5).

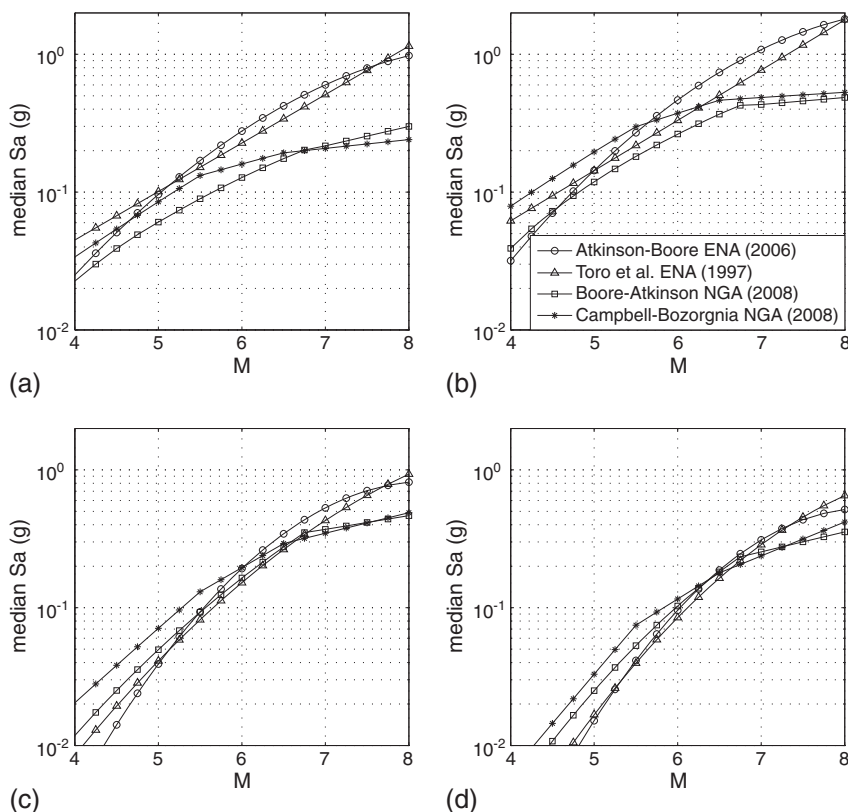


Figure 10. Median spectral acceleration as a function of magnitude (with constant distance of 15 km and V_{S30} of 310 m/s) as predicted by different GMPEs with (a) $T=0.0$ s (PGA), (b) $T=0.2$ s, (c) $T=0.6$ s, and (d) $T=1.0$ s.

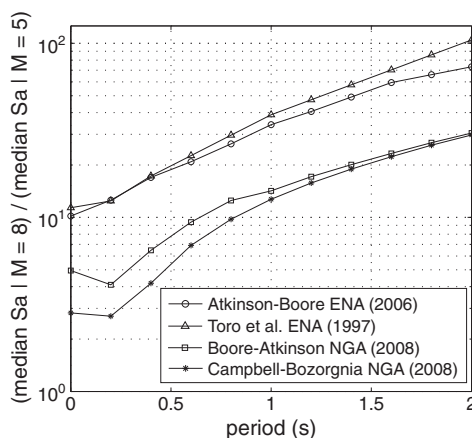


Figure 11. Ratio of predicted spectral acceleration for a magnitude 8 earthquake to a magnitude 5 earthquake plotted against period for different GMPEs (with constant distance of 15 km and V_{S30} of 310 m/s).

3.1. Gutenberg–Richter magnitudes

Figure 12 shows the deaggregation of magnitude and ϵ given that $PGA = 0.2g$, for the example site with a fixed site-to-source distance of 15 km, a GR distribution of magnitudes with $m_{min} = 5$, and the Atkinson–Boore ENA GMPE. For a given magnitude, there is only a single ϵ value where previously there was a distribution of ϵ values, allowing this figure to be turned into a two-dimensional plot as shown in Figure 13(a), where both the deaggregation probabilities and

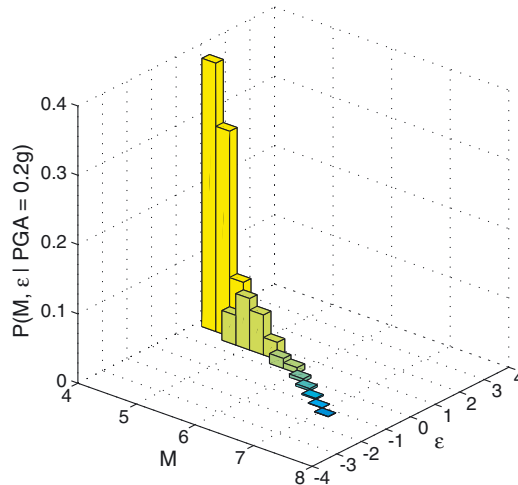


Figure 12. Magnitude and ϵ deaggregation given that $PGA = 0.2g$ for a site with fixed site-to-source distance of 15 km, GR distribution of magnitudes, and the Atkinson–Boore ENA GMPE.

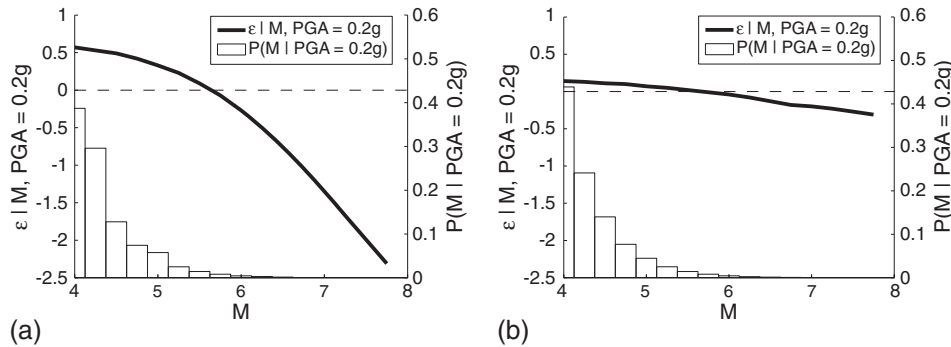


Figure 13. Two-dimensional representation of magnitude and ϵ deaggregations for a site with GR magnitude distribution and (a) the Atkinson–Boore ENA GMPE and (b) the Boore–Atkinson NGA GMPE.

corresponding ϵ values are plotted for each considered magnitude. The thick black line shows the ϵ deaggregation values as a function of magnitude, which is equivalent to the plan view of Figure 12. The thin dotted line shows where ϵ equals zero, so all ϵ values below this line are negative. The bars show the magnitude deaggregation, or the probability of observing a certain magnitude given that $PGA = 0.2g$. From the height of the bars, one can see how probable a given magnitude is, and thus how probable the associated ϵ is. For this case, we see that most of the probability content is clustered beneath the positive ϵ values, and while there is some probability of negative ϵ , it is very small. Figure 13(b) shows the deaggregation for a site with the same seismic source, but using the Boore–Atkinson NGA GMPE developed for the WUS. The magnitude deaggregation is very similar for both GMPEs, but the ϵ deaggregation changes dramatically. When using the ENA equation, the ϵ values have a large range from 0.5 to -2.5 ; but when using the WUS equation, the ϵ values remain close to zero and only range from 0.2 to -0.4 .

3.2. Gutenberg–Richter slope

The slope of the GR distribution of magnitudes (i.e., b in Equation (7)), has an effect on the rate of large magnitude earthquakes as discussed previously. By varying b , the magnitude deaggregation will change and so will the probability of negative ϵ . Figure 14 shows two-dimensional magnitude and ϵ deaggregations given PGA equal to $0.2g$ for a site with a fixed distance, GR magnitude distribution, and ENA GMPE. The only difference between the figures is the value of GR slope, with b equal to 0.5 and 1.5 in Figures 14(a) and (b), respectively.

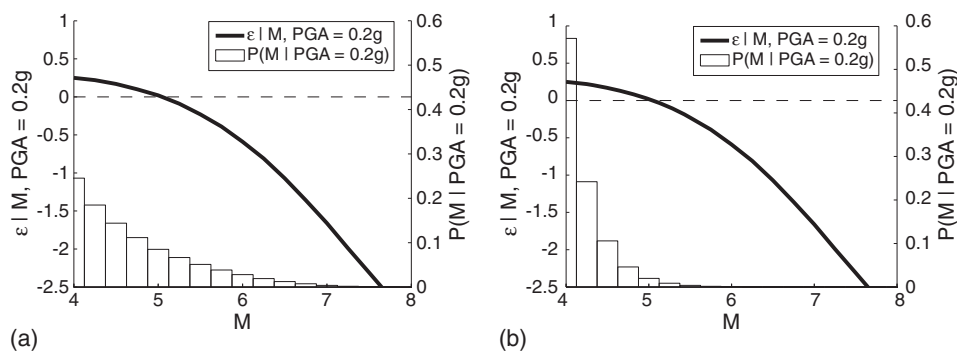


Figure 14. Two-dimensional magnitude and ε deaggregation with a GR distribution of magnitudes with (a) $b = 0.5$ and (b) $b = 1.5$.

In Figure 14, the ε values corresponding to each magnitude are exactly the same, but the magnitude deaggregation probabilities are different because the b value affects the probabilities of occurrence of the causal earthquakes. The small b used in Figure 14(a) implies that large magnitude earthquakes are more likely to occur and thus also more likely to cause $\text{PGA} = 0.2g$, while the opposite is the case in Figure 14(b). This means that a small b increases the probability of negative ε because it increases the frequency of large magnitude events. Large magnitude events cause negative ε to occur more frequently because they are capable of producing PGAs larger than the PGA amplitude of interest. A large b decreases the probability of negative ε because it decreases the frequency of large magnitudes.

Using these two-dimensional deaggregation figures, the probability of occurrence of negative ε can be computed for a given b and PGA. This probability is equal to the sum of the deaggregation probabilities associated with negative ε values, as shown in graphical form in Figure 15. The area within the shaded bars represents the probability of negative ε for this particular instance when b equals one and PGA equals $0.2g$. The probability of negative ε was computed for many different combinations of b and PGA, and is shown in Figure 16(a).

Figure 16(a) shows the GR b on one axis, PGA on another axis, and the probability of negative ε on the vertical axis computed using the Atkinson–Boore ENA GMPE. The largest probability of negative ε occurs at small b values and small PGAs. As PGA and b increase, the probability of negative ε decreases. These trends are consistent with all of the above results. Also recall that realistic values for b range from 0.8 to 1.2 and Figure 16(a) shows only a slight change in negative ε probability within this narrow range. Figure 16(b) shows the same plot computed with the Boore–Atkinson NGA GMPE, demonstrating a drastic decrease in the probability of negative ε because the WUS GMPE predicts lower PGAs. For PGA above $0.3g$, the probability of negative ε drops to zero regardless of the b value considered.

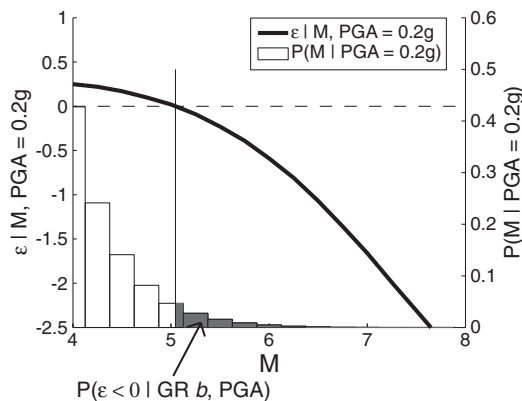


Figure 15. Graphical representation of the calculation for probability of occurrence of negative ε given GR b and PGA.

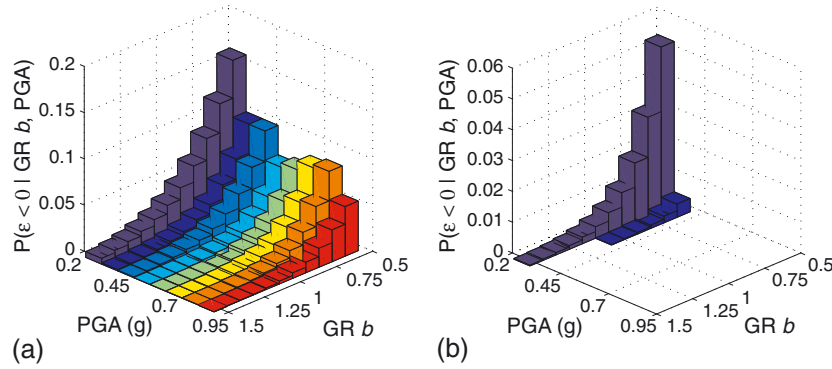


Figure 16. Probability of occurrence of negative ϵ given GR b and PGA using (a) the Atkinson–Boore ENA GMPE and (b) the Boore–Atkinson NGA GMPE. Note the change in vertical axis scale between the two figures.

We thus see that the GR slope has a slight effect on the probability of negative ϵ , but not in a significant way. The choice of GMPE and PGA amplitude play a more dominant role as demonstrated by the difference between Figures 16(a) and 16(b). Therefore, the effects of b on the occurrence of negative ϵ in deaggregation can be neglected, especially for sites located in the WUS.

3.3. Characteristic earthquakes

The next case considers a site with characteristic earthquakes (for consistency, the magnitudes, probabilities, and rate of the characteristic earthquakes are the same as those used in the above case studies in section 2.3, see Table I). Figure 17 shows deaggregations for this site using an ENA GMPE and a WUS GMPE, and is comparable to Figure 13 where a GR distribution was used.

The ϵ values associated with each magnitude remain the same whether the magnitude distribution model is GR or includes characteristic earthquakes (as can be seen by comparing Figures 13 and 17). However, the magnitude deaggregation probabilities change dramatically because large spikes of probability occur at the characteristic earthquakes. When an ENA GMPE is used, these spikes of probability correspond with large negative ϵ values, meaning that the probability of observing negative ϵ at a site located in ENA with characteristic earthquakes is very high. When a WUS GMPE is used, the probability spikes associated with characteristic earthquakes occur where ϵ is close to zero, so the likelihood of seeing large negative ϵ values remains small.

4. IMPLICATIONS FOR CONDITIONAL MEAN SPECTRUM CALCULATIONS

Recall that the motivation for doing these calculations was to understand the impact on CMS calculations. A negative ϵ value will invert the shape of the CMS, causing larger response spectra

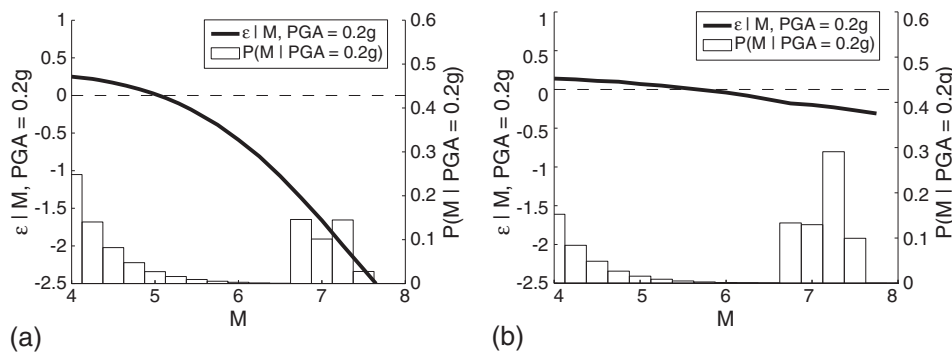


Figure 17. Two-dimensional magnitude and ϵ deaggregations for a site with characteristic earthquakes and using (a) the Atkinson–Boore ENA GMPE and (b) the Boore–Atkinson NGA GMPE.

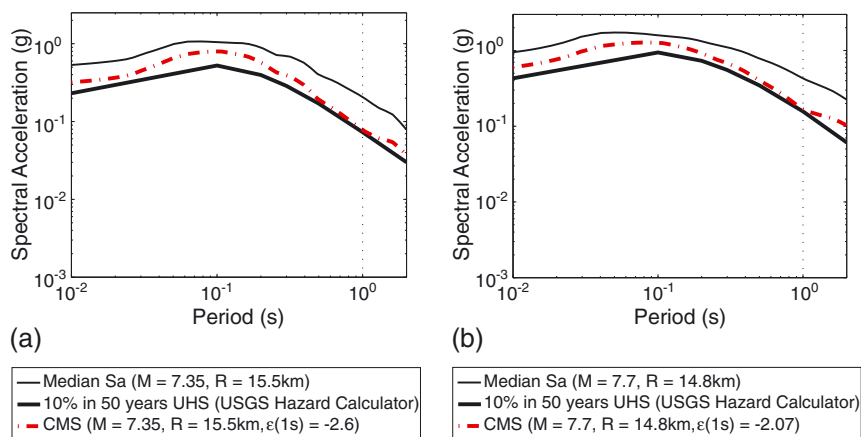


Figure 18. CMS computed using values from USGS deaggregation at an exceedance rate of 10% in 50 years for (a) Charleston, SC and (b) the NMSZ.

than the UHS at periods other than the conditioning period. Figure 18 shows the CMS computed for Charleston, SC (33.16°N , 80.2°W) and the NMSZ (36.58°N , 89.7°W) using modal deaggregation values from USGS for spectral acceleration at a period of 1 s and with a probability of exceedance of 10% in 50 years, which approximately corresponds to the ‘design basis earthquake’ level used by building codes. Because of variation in source models and numerical methods between the calculations in this paper and those performed by the USGS, the CMS in the following figure have been calculated by slightly adjusting the deaggregation ϵ so that the CMS computed using each model matches the UHS at the conditioning period. The median spectrum for the NMSZ was computed using a weighted combination of four GMPEs: Atkinson–Boore ENA GMPE with stress drop equal to 140 bar, Atkinson–Boore ENA GMPE with stress drop equal to 200 bar, Toro *et al.* ENA GMPE, and Somerville *et al.* ENA GMPE [19]. These are 4 of the 7 GMPEs used by the USGS to model the NMSZ, with weights taken from GMPE deaggregation provided by the USGS and normalized to sum to one. At the 2% probability of exceedance in 50 years level, which is approximately equal to the ‘maximum considered earthquake’ level used by building codes, the modal ϵ for spectral acceleration at a period of 1 s is 0.01 for Charleston, SC and 0.46 for the NMSZ.

These cases are associated with negative ϵ deaggregation values (because they are ENA sites with strong characteristic earthquake contributions to hazard), so the CMS predicts larger response spectra than the UHS. The typical argument that the UHS is conservative is clearly not valid at these sites and for these return periods. On the other hand, perhaps the UHS is unexpectedly unconservative in these cases, because the CMS aims to find an ‘expected’ spectrum and the UHS falls below that. Depending upon the circumstance, one might even decide that spectra associated with negative ϵ ’s should not be used for engineering design, whether in the UHS or CMS, because the resulting spectrum is smaller than the median spectrum associated with the causal magnitude and distance. In such cases, the median spectrum might serve as a practical design spectrum. In general, the best choice of target spectrum will depend upon the goals of the subsequent analysis, but it is informative to see these unexpected relationships between target spectra in the case of negative deaggregation ϵ ’s.

In Charleston, SC, the maximum predicted spectral acceleration amplitude at any period is 0.53g and 0.80g from the UHS and the CMS, respectively. In the NMSZ, the maximum predicted spectral acceleration amplitude is 0.94g and 1.28g from the UHS and the CMS, respectively. These amplitudes of spectral acceleration are significant and cannot be neglected in structural analysis, but they are well constrained to areas in ENA with characteristic earthquakes. Therefore, it is suggested that the potential effects of negative ϵ on target spectra computation need to be considered in these specific areas, but are effectively irrelevant elsewhere.

5. CONCLUSIONS

A set of case study probabilistic seismic hazard analysis calculations have been performed to identify circumstances under which hazard deaggregation results may have significant contributions from negative ε values. The ground motion parameter ε indicates the degree to which a ground motion's spectral acceleration amplitude is larger or smaller than the predicted median S_a , given the causal earthquake (defined by a magnitude, distance, etc.). In most seismic hazard calculations, which are performed to study exceedance of high amplitude (i.e., low probability of exceedance) S_a values for design checks and loss analyses, deaggregation ε values are positive, indicating that occurrence of the target S_a is likely to be caused by a ground motion whose S_a was unusually strong given its causal earthquake. Although likely to be rare, the occurrence of negative ε values is of interest because in those cases our conventional thinking about resulting Uniform Hazard Spectra (UHS) and Conditional Mean Spectra (CMS) is incorrect. The case studies considered here thus serve to help identify circumstances under which such cases might arise.

The case studies indicated that Ground Motion Prediction Equations calibrated for Eastern North America ground motions and special seismicity models are the most significant factors contributing to occurrence of negative deaggregation ε 's. A special seismicity model uses characteristic earthquakes or a Gutenberg-Richter (GR) distribution with a large minimum magnitude to describe the frequency of different earthquake magnitudes, while a typical seismicity model uses a GR distribution with a wide range of magnitudes to describe this frequency. The GMPE considered here for ENA predicts higher median PGA and short-period S_a values than models calibrated for the Western United States (WUS), resulting in more likely occurrence of negative ε 's given a particular PGA or S_a value. The existence of characteristic earthquakes also increases the occurrence of negative ε because large magnitude earthquakes are often capable of producing ground motions much larger than the PGA or S_a amplitude of interest. The combination of an ENA GMPE and special seismicity model creates the largest probability of negative ε . Special seismicity models occur in Eastern North America, in places such as Charleston, SC, the New Madrid Seismic Zone, eastern Tennessee, and a few locations in the Northeast US, leading to negative ε deaggregation values in the seismic hazard maps produced by the USGS for building and bridge design codes. Calculations considering typical GR magnitude distributions indicated that negative ε deaggregation values are unlikely to occur in such cases, and that variation in GR slopes had a much smaller impact on negative ε occurrence than the impact of GMPEs and special seismicity models.

These calculations indicate that there are indeed circumstances under which negative ε values arise in seismic hazard calculations. In these cases, the CMS predicts larger responses than the UHS, which is the opposite of the usual relationship between the two. It is notable, however, that negative ε 's are well constrained to areas in ENA with special seismicity, and their effect on target spectra may only need to be considered in these limited areas. This may lessen the practical worries about considering negative ε cases in anticipating trends in design spectra. It is also notable that negative ε 's tend to occur in areas near characteristic earthquake sources, and in such cases both the UHS and CMS are smaller in amplitude than the median spectrum associated with the characteristic earthquake; one might argue that in some design checking procedures it may be appropriate to use the larger median spectrum associated with those characteristic earthquakes rather than either the UHS or CMS. Such a decision would likely depend upon the intended goals of the analysis procedure.

REFERENCES

1. Baker JW. The Conditional Mean Spectrum: a tool for ground motion selection. *Journal of Structural Engineering* 2011; **137**(3):322–331.
2. Baker JW, Cornell CA. A vector-valued ground motion intensity measure consisting of spectral acceleration and epsilon. *Earthquake Engineering and Structural Dynamics* 2005; **34**(10):1193–1217.
3. Bazzurro P, Cornell CA. Disaggregation of Seismic Hazard. *Bulletin of the Seismological Society of America* 1999; **89**(2):501–520.
4. Bazzurro P. Probabilistic seismic demand analysis. PhD Thesis, Stanford, CA: Stanford University, 1998; 329.
5. Bommer JJ, Scott SG, Sarma SK. Hazard-consistent earthquake scenarios. *Soil Dynamics and Earthquake Engineering* 2000; **19**:219–231.

6. Naem F, Lew M. On the Use of Design Spectrum Compatible Time Histories. *Earthquake Spectra* 1995; **11**(1):111–127.
7. Reiter L. *Earthquake hazard analysis: Issues and insights*. Columbia University Press: New York, 1990.
8. Haselton CB, *et al.* Evaluation of Ground Motion Selection and Modification Methods: Predicting Median Interstory Drift Response of Buildings. PEER Technical Report 2009/01, Berkeley, California, 2009; 288.
9. Baker JW, Jayaram N. Correlation of spectral acceleration values from NGA ground motion models. *Earthquake Spectra* 2008; **24**(1):299–317.
10. Harmsen SC. Mean and Modal Epsilon in the Deaggregation of Probabilistic Ground Motion. *Bulletin of the Seismological Society of America* 2001; **91**(6):1537–1552.
11. Petersen MD, *et al.* Documentation for the 2008 update of the United States national seismic hazard maps. *US Geological Survey Open-File Report 2008–1128*, vol. **1128**, p. 61, 2008.
12. Atkinson GM, Boore DM. Earthquake ground-motion prediction equations for eastern North America. *Bulletin of the Seismological Society of America* 2006; **96**(6):2181.
13. Gutenberg B, Richter CF. Frequency of earthquakes in California. *Bulletin of the Seismological Society of America* 1944; **34**(4):185–188.
14. McCann MW, Reed JW. Lower bound earthquake magnitude for probabilistic seismic hazard evaluation. *Nuclear Engineering and Design* 1990; **123**:143–153.
15. Schwartz DP, Coppersmith KJ. Fault behavior and characteristic earthquakes: Examples from the Wasatch and San Andreas fault zones. *Journal of Geophysical Research* 1984; **89**(7):5681–5698.
16. Boore DM, Atkinson GM. Ground-Motion Prediction Equations for the Average Horizontal Component of PGA, PGV, and 5%-Damped PSA at Spectral Periods between 0.01 s and 10.0 s. *Earthquake Spectra* 2008; **24**(1):99–138.
17. Toro GR, Abrahamson NA, Schneider JF. Model of Strong Ground Motions from Earthquakes in Central and Eastern North America: Best Estimates and Uncertainties. *Seismological Research Letters* Feb. 1997; **68**(1):41–57.
18. Campbell KW, Bozorgnia Y. NGA Ground Motion Model for the Geometric Mean Horizontal Component of PGA, PGV, PGD and 5% Damped Linear Elastic Response Spectra for Periods Ranging from 0.01 to 10 s. *Earthquake Spectra* 2008; **24**(1):139–171.
19. Somerville P, Collins N, Abrahamson N, Graves R, Saikia C. Ground motion attenuation relations for the central and eastern United States. USGS Award Number: 99HQGR0098, 2001; 38.